processes

MDPI

Article

Optimizing Light Management in Bifacial Perovskite Solar Cells Using Silica-Based Anti-Dust and Anti-Reflection Coatings for Harsh Environments

Kevin Thomas [1], Ahasanur Rahman [1], Amith Khandakar [1], Puvaneswaran Chelvanathan [2], Brahim Aissa [3] and Mohammad Istiaque Hossain [3,*]

[1] Department of Electrical Engineering, College of Engineering, Qatar University, Doha 2713, Qatar; kt1908425@qu.edu.qa (K.T.); ar1904518@qu.edu.qa (A.R.); amitk@qu.edu.qa (A.K.)
[2] Solar Energy Research Institute (SERI), National University of Malaysia (UKM), Bangi 43600 UKM, Malaysia; cpuvaneswaran@ukm.edu.my
[3] Qatar Environment and Energy Research Institute (QEERI), Hamad Bin Khalifa University (HBKU), Qatar Foundation, Doha 5825, Qatar; baissa@hbku.edu.qa
* Correspondence: mhossain@hbku.edu.qa

Abstract: In this work, we demonstrate an advanced light management strategy for bifacial perovskite solar cells incorporating a silica-based anti-dust and anti-reflection (AR) coating. The silica layer provides dual functionality, enhancing optical efficiency through effective reflection suppression and protecting the solar cell surface from environmental contaminants, especially dust. The hydrophobic nature of the silica coating further prevents accumulation of dust and particulate matter, supporting a self-cleaning mechanism that maintains cell transparency and performance over extended periods. The simulation results indicated that transitioning from a monofacial to a bifacial design with a silica layer on top had a considerable impact on the PSC performance. The optimized bifacial structure demonstrated high-performance metrics, achieving a voltage of 1.35 V, a fill factor of 84.24%, a current density (J_{SC}) of 29.10 mA/cm^2, and a power conversion efficiency of 31.00% when illuminated from the electron transport layer side. When illuminated from the hole transport layer side, the structure attained an efficiency of 22.00% with a calculated bifaciality factor (BF) of 72.12%, highlighting the potential of bifacial PSC design. Our findings reveal that the addition of the silica layer led to a notable improvement in light harvesting efficiency.

Keywords: bifacial solar cell; perovskite solar cells; SCAPS-1D; silica layer; anti-dust coatings; anti-reflection coatings

check for updates

Academic Editor: Fabio Carniato

Received: 18 January 2025
Revised: 12 February 2025
Accepted: 17 February 2025
Published: 18 February 2025

Citation: Thomas, K.; Rahman, A.; Khandakar, A.; Chelvanathan, P.; Aissa, B.; Hossain, M.I. Optimizing Light Management in Bifacial Perovskite Solar Cells Using Silica-Based Anti-Dust and Anti-Reflection Coatings for Harsh Environments. *Processes* **2025**, *13*, 578. https://doi.org/10.3390/pr13020578

Copyright: © 2025 by the authors. Licensee MDPI, Basel, Switzerland. This article is an open access article distributed under the terms and conditions of the Creative Commons Attribution (CC BY) license (https://creativecommons.org/licenses/by/4.0/).

1. Introduction

In recent years, perovskite solar cells (PSCs) have attracted a lot of interest in solar cell research because of their quick development and potential for efficiency and cost-effectiveness. The first PSC in 2009 had a moderate efficiency of 3.8% [1,2], but in just ten years, the efficiency of methyl ammonium lead halide ($CH_3NH_3PbI_3$) perovskite-based cells [3] reached 23.7%. Perovskite materials' better absorption coefficient, reduced binding energy, carrier mobility, and diffusion length [4] make them suitable for photovoltaic applications. However, it is crucial to understand that certain lead-containing perovskite compounds, like $MAPbI_3$, raise concerns regarding stability and environmental impact, which may limit their widespread application in solar cell technology. One solution to this problem is the creation of bifacial structures that make use of superior optoelectronic

properties such as higher carrier transport, improved absorption efficiency, and a lower exciton binding energy [5]. Featuring a 1.3 eV direct bandgap, this bifacial design excels in absorption and belongs to a periodic table group with similar properties to its lead-based counterpart. A transparent glass substrate, contact electrodes, perovskite layer, hole transport layer, and electron transport layer make up the standard PSC structure, which is depicted in Figure 1. The bifacial structure of perovskite solar cells, when combined with a silica (SiO_2) layer on the front surface, enhances both the efficiency and durability of the cell. In a bifacial perovskite solar cell, light can enter from both the front and reverse sides, allowing additional light capture and energy generation by utilizing light reflected from surrounding surfaces. The integration of a SiO_2 layer on the front surface provides an anti-reflective coating, reducing incident light reflection and increasing light transmission into the active layers. This silica layer also acts as a protective barrier, improving the cell's stability by shielding the perovskite layer from environmental factors like moisture, UV exposure, and airborne particles. By reducing surface reflections, the SiO_2 layer ensures that a greater proportion of incoming light is absorbed by the perovskite layer, boosting the overall power conversion efficiency and the short-circuit current density (Jsc) of the cell. By enhancing front-side light capture, the bifacial design maximizes performance under diffused and reflected light conditions, making it particularly advantageous under varied environmental conditions. Together, the bifacial architecture and the SiO_2 anti-reflective layer contribute to a highly efficient and stable perovskite solar cell, suitable for both rooftop installations and integrated photovoltaic applications where maximum utilization of light is essential. While the proposed silica-based anti-dust and anti-reflection coatings demonstrate promising optical and self-cleaning properties, their long-term stability under real-world conditions remains insufficiently explored. Factors such as exposure to extreme temperatures, humidity, UV radiation, and mechanical stress can impact the durability and performance of the silica layer over extended operational periods. Detailed investigation into these coatings' structural integrity, adhesion strength, and resistance to environmental degradation is crucial for ensuring their reliability in harsh environments. Furthermore, additional characterization of the material properties, including refractive index, porosity, surface roughness, and thermal stability, is necessary to optimize the coatings' integration with bifacial perovskite solar cells. A thorough understanding of these aspects will contribute to the development of robust and efficient light management strategies for sustainable photovoltaic applications. The impact of environmental factors such as dust accumulation, UV degradation, and mechanical stress on the long-term performance of these coatings has not been adequately addressed in the literature. This manuscript seeks to fill this gap by proposing a silica-based anti-dust and anti-reflection coating that not only enhances light management but also offers protection against dust buildup, improving the overall stability and efficiency of bifacial perovskite solar cells under real-world conditions. This paper bridges these gaps through a comprehensive investigation that used both experimental and numerical approaches to optimize the coating properties, assess the impact on device performance, and evaluate the long-term durability of the proposed solution. By combining these functionalities, this study aims to advance the practical application of perovskite solar cells in harsh environments, offering a more sustainable and efficient solution for next-generation photovoltaic technologies.

The electron transport layer (ETL) works as a hole-blocking layer [6], which helps prevent charge recombination. Titanium dioxide (TiO_2) is favorable due to its transport mobility, stability, bandgap alignment, and adaptability to various deposition methods [7]. The hole transport layer (HTL), on the other hand, functions as an electron-blocking layer that prevents electron flow while encouraging hole transport [8]. Perovskite solar cells are becoming more and more necessary for vehicles as well as for building integrated

photovoltaics. Conventional or tandem structures are becoming less common because of this demand. Adopting a bifacial design is becoming a more practical solution instead.

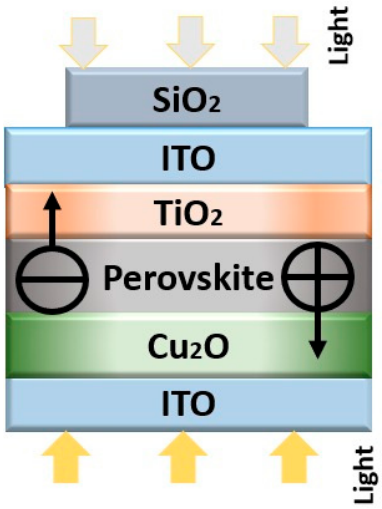


Figure 1. SiO_2/ITO/TiO_2/perovskite/copper oxide/ITO device structure.

The critical factors impacting PSCs' performance are their ability to effectively manage incident light, allowing maximum photon absorption while minimizing losses from reflection. Anti-reflective coatings (ARCs) have been extensively studied and used to reduce the reflectance at the surface of solar cells. Traditionally, magnesium fluoride (MgF_2) has been employed as an ARC material in PSCs because of its low refractive index (~1.38) and wide spectral coverage, effectively reducing reflection losses across a broad range of wavelengths [9]. MgF_2 coatings, typically implemented in simulations using SCAPS-1D, have demonstrated notable improvements in light management and device optimization, with recent studies showing efficiency of up to 21.62% for MgF_2-coated perovskite structures [10]. Despite these successes, the optical properties of MgF_2 are not ideally matched for all PSC materials, which has led to continued research into alternative ARCs that could provide superior light management.

Silicon dioxide (SiO_2) has a refractive index of approximately 1.5 and has recently emerged as a promising ARC candidate for PSC applications. Unlike MgF_2, SiO_2 offers better compatibility with certain perovskite layers and provides the potential for enhanced constructive and destructive interference, allowing further optimization of light absorption [11]. SiO_2 coatings can be engineered to achieve the ideal balance between reflection minimization and transmission optimization, particularly for specific wavelengths that are crucial for PSC operation. Additionally, the robustness and environmental stability of SiO_2 provide significant advantages in maintaining device performance over time, especially under variable climatic conditions [12,13]. This work distinguishes itself from previous research on light management strategies in solar cells by specifically focusing on the dual functionality of silica-based coatings that provide both anti-dust and anti-reflection properties to bifacial perovskite solar cells operating in harsh environments. While conventional studies have primarily optimized anti-reflection layers to enhance optical absorption or explore self-cleaning surfaces separately, our approach integrates these functionalities into a single coating, improving long-term performance and environmental resilience. Additionally, this research evaluated the stability of the silica layer under real-world conditions, considering factors such as UV degradation, mechanical wear, and thermal cycling—areas often overlooked in prior studies. Through experimental characterization and numerical simulations, we provide a comprehensive analysis of how silica coatings influence optical performance, light-trapping efficiency, and resistance against surface contamination,

contributing to the development of more durable and efficient solar cells for challenging deployment scenarios.

Previous studies have demonstrated that ARCs can significantly affect the efficiency of PSCs by reducing surface reflection and improving photon utilization [14]. However, most prior research, particularly studies relying on SCAPS-1D simulations, assumed either zero reflectance or employed default settings that failed to accurately account for the wavelength-dependent nature of light's interaction with the ARC layer [10]. Such oversimplifications often lead to discrepancies between simulated and experimental results, thereby limiting the accuracy of predictive models of PSC performance. This study aims to bridge that gap by implementing a wavelength-dependent reflectance model for SiO_2 as an ARC for PSCs, as shown in Figure 1, specifically focusing on perovskite structures that have demonstrated compatibility with SiO_2 coatings. The need to progress performance and stability in PSCs for applications like building-integrated photovoltaics (BIPV) and vehicle-integrated photovoltaics (VIPV) underscores that tandem or conventional structures need to be switched to a bifacial structure. By addressing stability and environmental issues and offering substitutes for conventional materials, this study investigates new materials such as copper oxide as possible HTMs. We can learn more about the viability of this type of solar panel by combining them all to observe the performance of perovskite solar panels. By enabling the absorption of more photons, thick absorber layers improve light absorption. Nevertheless, the carrier diffusion length increases, leading to higher recombination rates and transit times due to charge extraction pathways not being optimized. The efficiency of light absorption and the charge extraction are both impacted by the bifacial structure's design, which includes the configuration of layers and interfaces.

Prioritizing one component over another in design decisions can disturb other aspects of the design, highlighting the need for careful optimization methods. By absorbing more sunlight, increasing light absorption usually results in a higher energy yield. Increasing the efficiency of charge extraction through modification by adding more contacts or layers compromises the bifacial structure's visual transparency, particularly in building-integrated photovoltaics (BIPV). To guarantee commercial viability, trade-offs between pragmatic considerations and performance enhancements must be carefully assessed. Electrons can move around the device efficiently because metal oxides often have high electron mobility [3]. This improves overall device performance, reduces recombination losses, and expedites charge carrier extraction. Metal oxides' energy levels can be altered by dopants or compositional shifts to bring them into line with those of neighboring layers of solar cell. This alignment lowers energy loss at the interfaces and improves charge carrier extraction. Additionally, under normal operating conditions, metal oxides are typically chemically stable and do not degrade when exposed to light, oxygen, or moisture. This stability adds to the solar cells' long-term dependability and robustness.

Implementing the proposed silica-based anti-dust and anti-reflection coating in practical research settings presents several challenges and potential trade-offs. One of the main limitations is the long-term durability of the silica layer under harsh environmental conditions. While silica coatings are promising for the management of dust and reflection, their resistance to factors like UV degradation, mechanical abrasion, and thermal cycling may degrade over time, affecting their overall efficiency and effectiveness. Additionally, the manufacturing process of applying a uniform and stable silica layer across large-scale modules could be challenging, especially if high precision is required for optimal light management and long-lasting performance. Another potential trade-off is the balance between the anti-reflection properties and the anti-dust functionality, whereby enhancing one property may inadvertently affect the other. For example, a highly hydrophobic silica surface that repels dust may also influence the coating's ability to maintain optical

transparency, potentially diminishing its anti-reflection efficiency. Lastly, the increased complexity of integrating the silica coating with perovskite absorber layers may introduce additional interfaces that could affect carrier transport or introduce defects, thus influencing the overall performance of the device. These factors should be carefully considered and addressed in future studies, to optimize the balance between performance and practicality.

Fluorine-doped tin oxide (FTO) and indium tin oxide (ITO) are transparent conductive oxides with high optical transparency and electrical conductivity. Because of this combination, they can function as transparent conductive electrodes that effectively collect charge carriers while allowing light to pass through the active layer. Due to their affordability and abundance, metal oxides are desirable raw materials for the manufacture of solar cells on a large scale. Their accessibility lowers the total cost of producing solar panels, increasing the technology's economic feasibility. Metal oxides can perform a variety of tasks in a solar cell, including hole blocking, electron transport, and in some kinds of photovoltaic devices, active layer participation. Because of their adaptability, unique device architectures that meet performance requirements can be created. To overcome these issues, this work explores the use of TiO_2 as electron transport layer and copper oxide as hole transport layer in bifacial PSC. Numerous simulations were carried out with SCAPS, examining different parameters in each PSC layer and the direct process of fabrication. To assess the performance of each layer (HTL, Abs, and ETL), critical parameters such as fill factor (FF), power conversion efficiency, open-circuit voltage (V_{OC}), and short-circuit current (J_{SC}) were analyzed. This study examined operating temperature, doping concentration, thickness, type, and defect density to identify the optimal configurations under SiO_2 coating. Furthermore, PSC performance was examined under various concentrations of incoming light through numerical analyses conducted with the SCAPS simulator under AM1.5G light conditions. The transmission option in SCAPS was used in these simulations to adjust the incoming light's intensity. By altering the transmission coefficient, this option enabled the simulation of various light conditions.

2. Materials and Methods

SCAPS version 3.3.11 (Solar Cell Capacitance Simulator) is widely used for simulating the impact of structural and material parameters on the performance of perovskite solar cells (PSCs)e. One key parameter studied through SCAPS is the effect of increasing the perovskite layer's thickness on overall device efficiency. As the thickness of the perovskite absorber layer increases, there is generally an initial improvement in the cells' light absorption, which enhances the short-circuit current density (Jsc) due to the capture of more incident photons. However, this improvement plateaus and may eventually reverse at higher thicknesses, where issues such as increased bulk recombination, longer distances for carrier diffusion, and reduced efficiency of charge extraction begin to offset the gains in light absorption. Excessive thickness can also lead to a drop in the open-circuit voltage (Voc), as charge carriers may recombine before reaching the respective electrodes. SCAPS simulations often reveal an optimal thickness range where the balance between light absorption and charge transport is maximized, resulting in peak power conversion efficiency. Through this approach, SCAPS enables systematic exploration and optimization of the PSCs' thickness to improve cell efficiency while avoiding material waste and ensuring practical manufacturability.

SCAPS-1D version 3.3.11, developed in ELIS at the University of Gent, was used in this work [15]. The software uses the continuity equation as well as the Poisson Equation (1):

$$\frac{d}{dx}\left(-\varepsilon(x)\frac{d\varphi}{dx}\right) = q\left[p(x) - n(x) + N_D^+(x) - N_A^-(x) + p_t(x) - n_t(x)\right] \quad (1)$$

$$\frac{dp_n}{dt} = G_p - \frac{p_n - p_{n0}}{\tau_p} + p_n \mu_p \frac{d\xi}{dx} + \mu_p \xi \frac{dp_n}{dx} + D_p \frac{d^2 p_n}{dx^2} \quad (2)$$

$$\frac{dn_p}{dt} = G_n - \frac{n_p - n_{p0}}{\tau_n} + n_p \mu_n \frac{d\xi}{dx} + \mu_n \xi \frac{dn_p}{dx} + D_n \frac{d^2 n_p}{dx^2} \quad (3)$$

where G stands for generation rate, τn and τp for the electron and hole lifetimes, respectively. The diffusion coefficient and electron charge are D and q, respectively. The electrostatic potential is represented by Ψ, and the electron and hole mobilities are represented by μp and μn. Concentrations of holes and free electrons are denoted by p(x) and m(x), while trapped holes and electrons are pt(x) and nt(x). The concentrations of ionized acceptors and donors are represented by N − D(x) and N + A(x), the electric field by ξ, and the direction along the thickness by x [16].

For this investigation, a conventional structure and an optimized two-stage PSC model device with backlighting were developed. The conventional device structure utilized in this work, ITO/copper oxide/Perovskite/TiO_2/ITO/SiO_2, represented the initial stage of optimizing the PSC device structure. The optimization process primarily focused on the TiO_2 layer while also examining other empirical properties such as operating temperature, layer thickness, and defects. Concurrent optimization of the perovskite layer, back contact layers, and hole transport layer involved examining different thicknesses [17–37].

Then, with dark currents present, the optimized structural design was investigated. The study also examined the effects of doping and the density of defects in the absorber layer on the PSCs' efficiency. To run the simulation, 1.5 G AM air mass illumination per square meter was used. In this study, each layer was optimized according to the efficiency analysis of the PSCs. The optimization of the ETL was the first step in the optimization process, which involved simulations with various thicknesses, defect densities, and operating temperatures. After that, the thickness of the absorber layer was tuned, ranging from 100 to 1000 nm. An optimized device structure was used to conduct and analyze the dark current. The impact of doping concentration and defect density on the recombination rate and performance of the absorber layer was also examined. Defect density and doping concentration in the absorber layer were altered from 10^{14} to 10^{18} cm^{-3}, respectively. Enhancing the reliability and efficiency of solar cells requires an understanding of and ability to control defect density. Increased density of defects may result in more charge carrier recombination, which lowers the device's overall efficiency. To provide a clearer understanding of recombination mechanisms affecting device performance, we distinguish between defect-assisted recombination and band-to-band recombination in bifacial perovskite solar cells. Defect-assisted recombination, primarily occurring through Shockley–Read–Hall (SRH) processes, is mediated by trap states within the perovskite bandgap, which capture and release charge carriers, leading to non-radiative energy loss. This mechanism is particularly detrimental in highly defective or poorly passivated films, significantly reducing open-circuit voltage (Voc) and fill factor (FF). In contrast, band-to-band recombination involves direct electron–hole recombination across the conduction and valence bands, typically leading to radiative emission. While intrinsic to semiconductor operation, excessive band-to-band recombination can still lower efficiency by reducing charge extraction before carrier collection. Using SCAPS-1D simulations, we analyzed these recombination pathways under different doping levels and material conditions, providing numerical and graphical insights into their respective contributions to performance losses. Understanding and mitigating defect-assisted recombination while controlling band-to-band recombination is crucial for optimizing the efficiency and stability of perovskite solar cells.

Defects can also create trap states in the semiconductor's bandgap, which can impede the transport and collection of charge carriers and impair device performance even more. Researchers can evaluate the effects of various defect configurations on device performance by adjusting simulation parameters associated with defect density, such as defect energy levels or trap state concentrations. Fill factor, open-circuit voltage, and short-circuit current are the components of these variables. Researchers can also create passivation and defect mitigation strategies by examining the relationship between device performance and defect density. Methods like material purification, surface passivation, and defect engineering can be beneficial, leading to decreases in defect densities and increasing the efficiency and dependability of solar cells. In conclusion, defect density is essential for comprehending and maximizing the performance of photovoltaic devices. Researchers can learn more about how defects affect device behavior and create plans to lessen their effects by integrating defect density data into analyses and simulations, which will ultimately increase the reliability and efficiency of solar cells.

3. Results

3.1. Layer Thickness Optimization

Optimization of layer thickness is covered in this section, with reference to the hole transport layer and electron transport layer. The thicknesses of the electron transport layer and hole transport layer in the specific instance described were 140 nm and 200 nm, in accordance with suggestions from previous research [1]. The simulation's operating parameters are displayed in Table 1.

Table 1. Values used to run the simulation.

Parameters	Layer Material			
	TiO_2	**SiO_2**	**Copper Oxide**	**Perovskite**
Bandgap (eV)	3.260	6.300	2.200	1.500
Electron Thermal Velocity (cm/s)	1.007×10^7	1.007×10^7	1.007×10^7	1.007×10^7
Electron affinity (eV)	4.000	3.200	3.200	3.900
Dielectric permittivity	10.000	3.900	9.400	10.000
CB ($1/cm^3$)	2.00×10^{18}	2.02×10^{17}	8.00×10^{17}	2.00×10^{18}
VB ($1/cm^3$)	1.80×10^{18}	1.20×10^{19}	1.80×10^{19}	1.80×10^{18}
Electron Mobility (cm^2/Vs)	2.000×10^2	6.250×10^1	2.000×10^2	2.000×10^2
Hole Thermal Velocity (cm/s)	1.000×10^2	1.000×10^2	1.000×10^7	1.000×10^2
Hole Mobility (cm^2/Vs)	2.500×10^1	0.800×10^1	1.000×10^2	1.000×10^1
CB ($1/cm^3$)	2.00×10^{18}	2.02×10^{17}	8.00×10^{17}	2.00×10^{18}
VB ($1/cm^3$)	1.800×10^{18}	1.10×10^{19}	1.800×10^{19}	1.800×10^{18}

The latter thickness was chosen for several reasons after it was discovered that a thickness of 500 nm had a higher short-circuit current (J_{SC}) and power conversion efficiency than a thickness of 1000 nm. The larger active layer was used to maximize charge production and improve the device's light-absorbing capabilities. Performance gains diminished after this thickness because important parameters like short-circuit current became saturated. Relationships between the thickness of the absorber layer and performance metrics are shown in Figures 2 and 3.

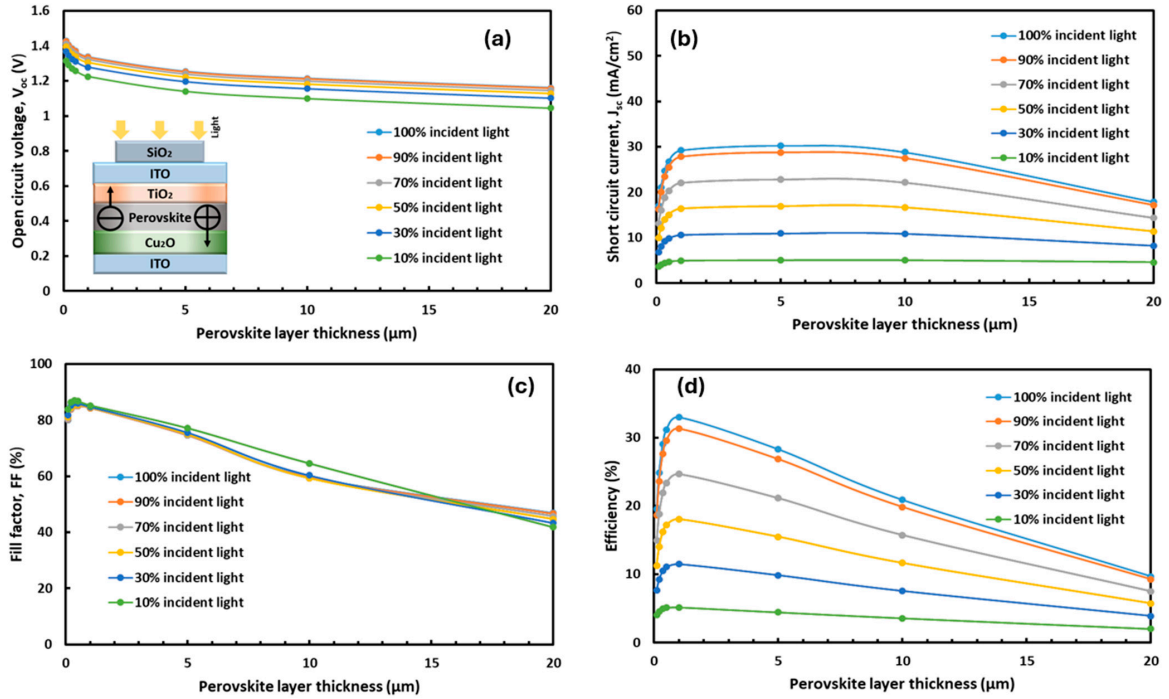


Figure 2. Performance variation in perovskite solar cells with the incident solar spectrum from the ETL side, in the range of 100–20,000 nm of absorber layer thickness. The variables include (**a**) open-circuit voltage (Voc), (**b**) short-circuit current (Jsc), (**c**) fill factor (FF), and (**d**) efficiency.

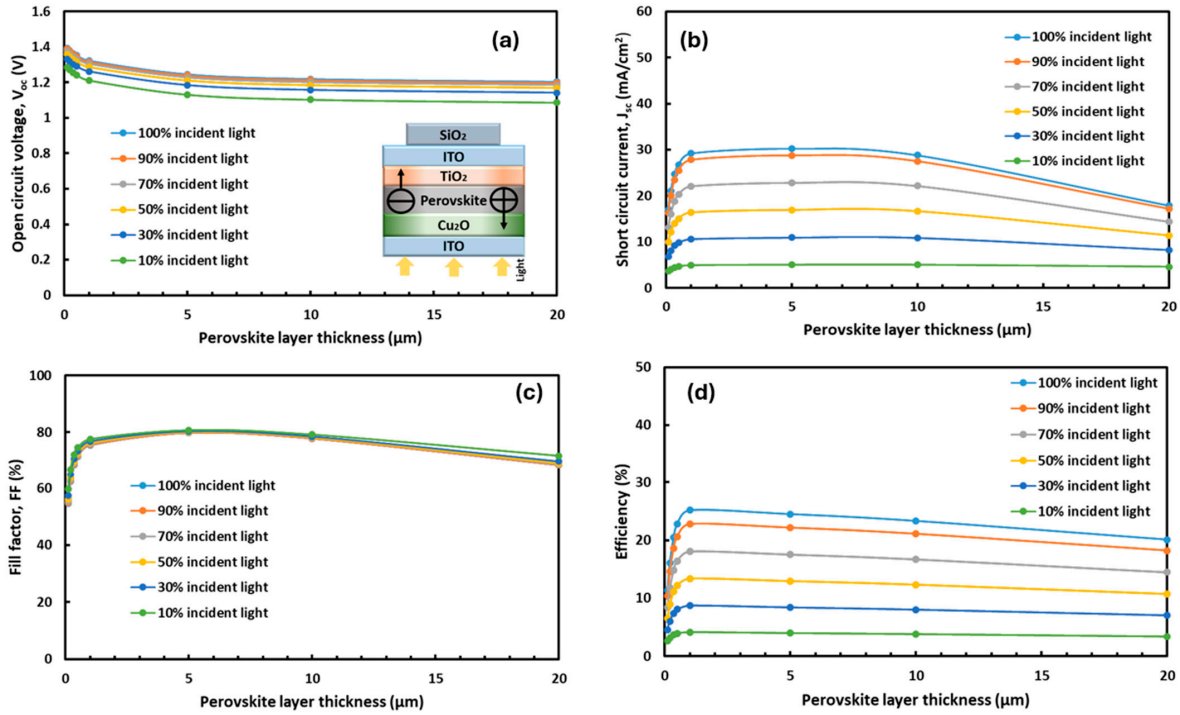


Figure 3. Performance variation in perovskite solar cell for the incident solar spectrum from the HTL side in the range of 100–20,000 nm of absorber layer thickness. The variables include (**a**) open-circuit voltage (Voc), (**b**) short-circuit current (Jsc), (**c**) fill factor (FF), and (**d**) efficiency.

3.2. Effects of Operating Temperature on Bifacial Solar Cells

A comparative study of bifacial perovskite solar cells was conducted with incident light from both the front and reverse sides to assess how performance was impacted, as shown in Figures 4 and 5. The operational temperature range considered for this analysis spanned

from 300 K to 400 K. As the results indicate, a rise in operating temperature generally led to a decline in cell efficiency. This was attributed to the temperature-dependent changes in key parameters such as carrier concentration, band gap, and electron and hole mobility, which tend to vary at elevated temperatures.

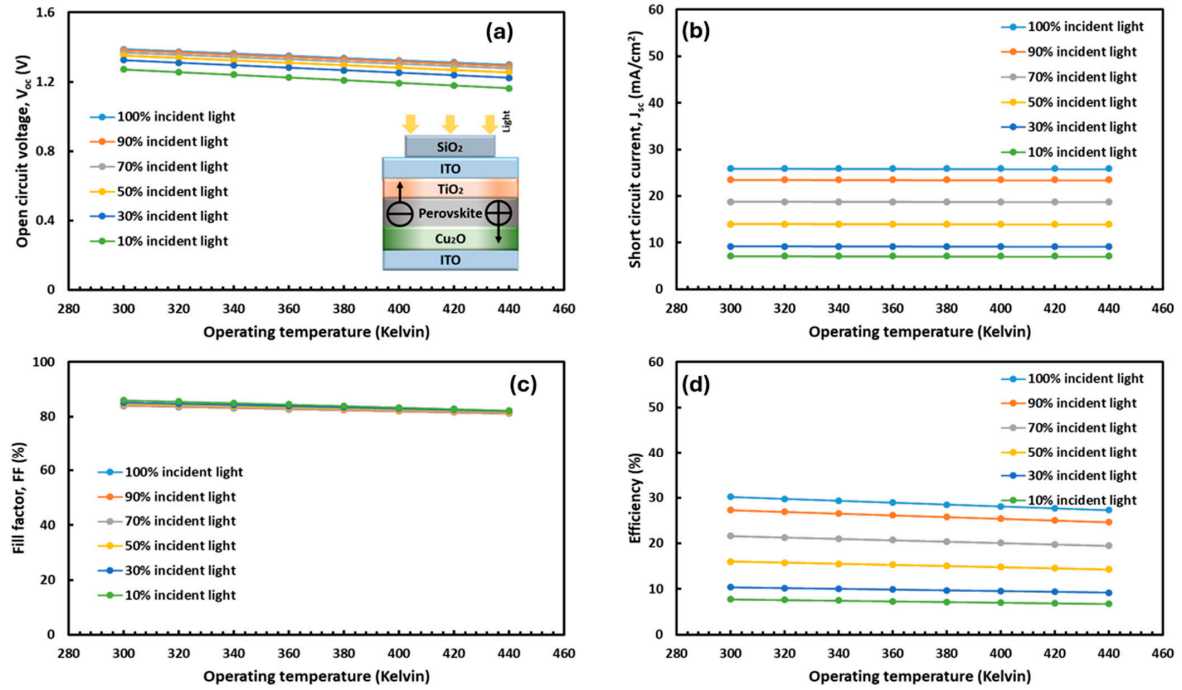


Figure 4. Performance of the device with the incident solar spectrum from the ETL side at different operating temperatures, at an absorber layer thickness of 350 nm: (**a**) open-circuit voltage (Voc), (**b**) short-circuit current (Jsc), (**c**) fill factor (FF), and (**d**) efficiency of perovskite solar cells.

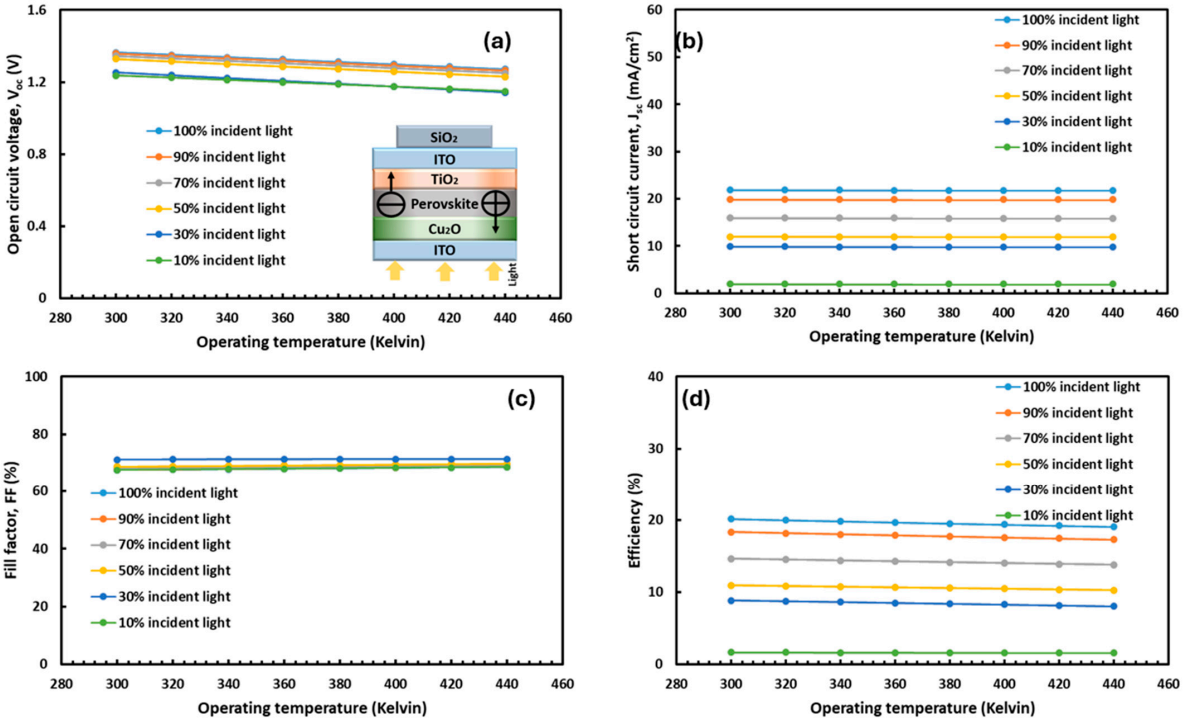


Figure 5. Performance of the device with the incident solar spectrum from the ETL side at different operating temperatures, at an absorber layer thickness of 350 nm: (**a**) open-circuit voltage (Voc), (**b**) short-circuit current (Jsc), (**c**) fill factor (FF), and (**d**) efficiency of perovskite solar cells.

3.3. Effects of Doping Concentration on TiO_2 Electron Transport Layers

The performance of bifacial solar cells was examined with various doping concentrations in the electron transport layer, as shown in Figure 6.

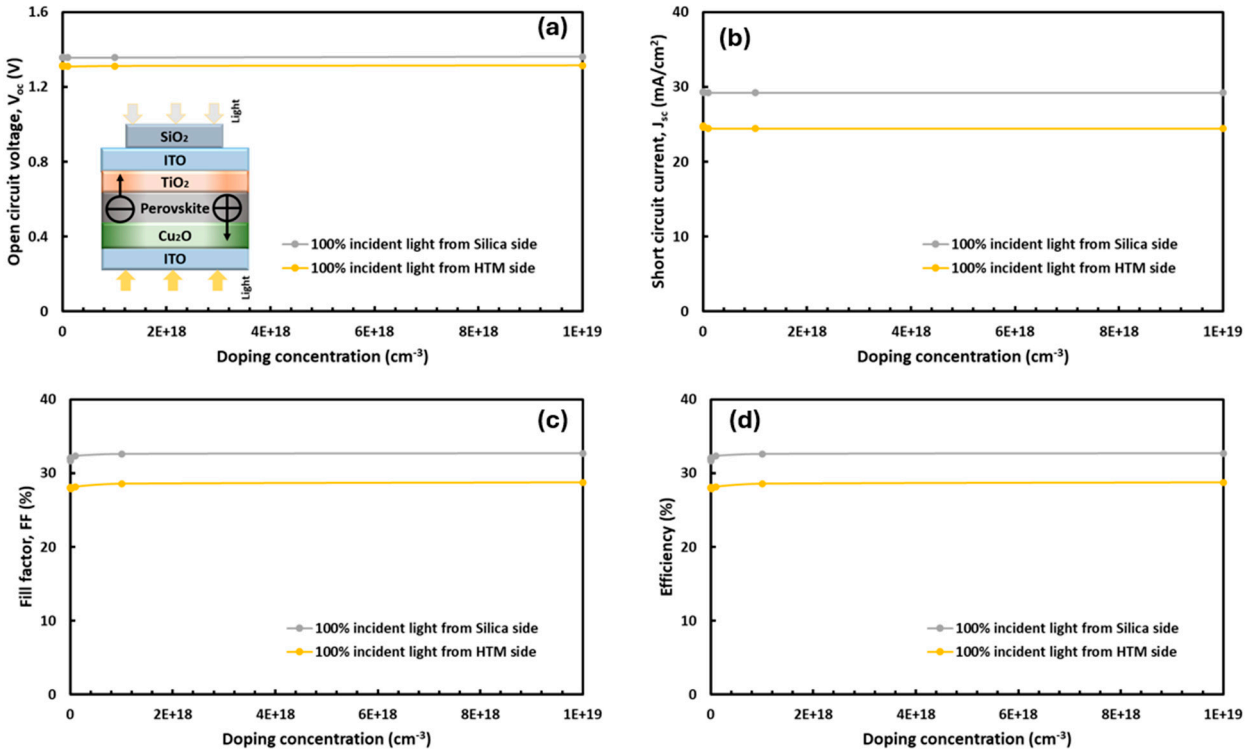


Figure 6. Variations in the performance of solar cells within the absorber layer thickness range of 350 nm for different TiO_2 ETL doping concentrations: (**a**) open-circuit voltage (Voc), (**b**) short-circuit current (Jsc), (**c**) fill factor (FF), and (**d**) efficiency (η) of perovskite solar cells.

4. Discussion

The above findings highlight the influence of layer thickness, operating temperature, and ETL doping concentration on the perovskite solar cells' performance.

4.1. Layer Thickness Optimization

The analysis revealed that an absorber layer thickness of 500 nm yielded higher short-circuit current density (Jsc) and power conversion efficiency compared with 1000 nm. Difficulties with defect management and material uniformity may have been the cause of the modest decline in efficiency seen beyond 1000 nm. It is important to keep in mind that even though these ideal thickness values were demonstrated advantageous under the conditions examined in this investigation, they may not be suitable for other configurations, and more investigation is needed to find out. Using SCAPS, we examined the effects of the thickness of the absorber layer, ranging from 100 to 20,000 nm, on important factors influencing the efficiency of solar cells. Figure 2 reveals that in all cell types, when the thickness of the absorber layer increased, the short-circuit current increased as well, peaking at about 1000 nm and then plateauing. After the incident photons were completely absorbed, the highest current was then generated, causing a slight drop (Figure 2b). After eliminating defect-assisted carrier recombination, the band-to-band recombination rate reduced performance beyond 1000 nm.

The following equation applies:

$$U\left(cm^{-3}\cdot s^{-1}\right) = B\left(np - n_i^2\right) \quad (4)$$

where the carrier densities under excitation are denoted by p and n, B is a constant unique to perovskites, and ni is the intrinsic density. We used the GaAs constant B (6.2×10^{-10} $cm^{-3} \cdot s^{-1}$) with a 1.43 eV direct gap, because no measured value was available. The fill factor remained constant as the thickness increased above 1000 nm, but the efficiency and Voc clearly declined, as shown in Figure 2d. These results imply that the thickness of the perovskite layer affected the PSCs' performance. As the perovskite thickness exceeded 300 nm, the Voc sharply dropped due to increased recombination leading to insufficient charge carrier separation at the interface between the absorber layer and the electron transport layer. This insufficient separation of charge carriers, which can also be brought on by higher series resistances, may cause Jsc to progressively drop. On the other hand, the TiO_2 layer functions as both a hole-blocking and electrically conductive layer while avoiding hole attachment, which makes it easier to collect electrons in the absorber layer. Since the TiO_2 layer is electrically conductive, its electrical conductivity is directly influenced by its thickness. The reported performance metrics including open-circuit voltage (Voc), fill factor (FF), short-circuit current density (Jsc), and power conversion efficiency are promising but need to be compared with those for other state-of-the-art perovskite solar cell (PSC) designs to assess their competitiveness. In our study, the integration of silica-based anti-dust and anti-reflection coatings improved light absorption and charge collection, resulting in notable enhancements in Voc and Jsc. However, compared with state-of-the-art PSCs that typically exhibit efficiency upwards of 20–25% for single-junction devices, our simulated efficiency may be lower, especially if the silica coating's impact on light management or carrier transport is not fully optimized. Furthermore, the fill factor (FF) observed in our study may show slight reductions compared with optimized PSC designs with advanced charge transport layers or interface engineering. The efficiency gains from the silica coating must be balanced against any potential loss in performance due to factors like increased series resistance or reduced efficiency of charge collection. Nonetheless, our results still demonstrate that silica-based coatings offer significant advantages in terms of environmental stability, dust resistance, and long-term durability—traits that are often overlooked in traditional performance comparisons but crucial for real-world applications in harsh environments. Further optimization and integration with other advanced materials could improve these performance metrics to bring them in line with the highest-performing PSC designs.

Increased photon absorption at the electron transport layer causes the electrical conductivity of the growing TiO_2 layer to drop, lowering the PSCs' performance over time by raising the charge transfer resistance. We kept the electron transport layer and hole transport layer at fixed thickness values, due to considerations unique to the bifacial cell design. When the recombination constant B is small, the saturation of both Jsc and Voc is visible beyond a thickness of 1000 nm, and when B is larger, it decreases, resulting in subsequent saturation of efficiency. Interestingly, for thicker perovskite layers, the decline in Voc was more pronounced than that in the short-circuit current. Understanding Voc's reliance on Jsc and the device's saturation current, J0, which is influenced by layer thickness, helps to understand this occurrence.

$$V_{oc} = \frac{kT}{e} Ln\left[\frac{I_{sc}}{J_0} + 1\right] \quad (5)$$

The device's dependence on its J0 saturation current is a major factor causing variation in the open-circuit voltage (Voc). Figure 3c makes it evident that the fill factor (FF) remained relatively constant even when the absorber's thickness changed. Given that the incident light's fill factor from the electron transport layer side is comparable to that of other devices, the bifacial device's high V_{OC} and J_{SC} could be the main factors contributing to its superior

efficiency. According to calculations, changes in the thickness of the solar cell layers have an impact on light transmission, which in turn affects bifaciality [17,18]. A crucial statistic for describing bifacial solar cells is the bifaciality factor, which is the ratio of rear side's efficiency to the front side's efficiency. The module's minimal power output, measured in kilowatt peak (kWp), is divided by the surface area, measured in square meters (m^2), to establish minimal efficiency.

4.2. Effects of Operating Temperature on Bifacial Solar Cells

The results in Figures 4 and 5 indicate that the rise in operating temperature generally led to a decline in cell efficiency. This was attributed to the temperature-dependent changes in key parameters such as carrier concentration, band gap, and electron and hole mobility, which tended to vary at elevated temperatures. Temperature-induced degradation in perovskite solar cells (PSCs) is a critical factor impacting device stability and performance, especially under prolonged exposure to sunlight. Elevated temperatures can lead to phase instability in the perovskite layer, accelerating decomposition and ion migration, which degrades cell efficiency over time. Incorporating a silica (SiO_2) anti-reflection coating (ARC) can help mitigate these effects. Being thermally stable and possessing excellent optical properties, SiO_2 not only enhances light absorption by reducing reflection but also provides a protective layer that moderates the temperature rise within the PSC structure. This thermal buffering effect helps preserve the structural integrity of the perovskite layer by limiting direct thermal stress. Additionally, SiO_2's hydrophobic nature provides a barrier against moisture ingress, which, in combination with temperature, often accelerates degradation. Studies have shown that PSCs with SiO_2 coatings maintain efficiency better than their uncoated counterparts in high-temperature environments, highlighting SiO_2's role as an effective ARC and stabilizer, contributing to the overall longevity and reliability of perovskite-based solar cells.

4.3. Effects of Doping Concentration on the TiO_2 Electron Transport Layer

The perovskite absorber layer of 1000 nm thickness was consistently associated with highest efficiency. While the fill factor remained constant, efficiency and open-circuit voltage (Voc) both sharply declined when the device was illuminated from the hole transport layer side, as seen in Figure 6. Changes in doping concentration were crucial for controlling recombination and carrier transport, leading to notable variations in EQE, especially in transport layers like TiO_2. Compared with experiments, simulations have certain limitations. Simulations primarily offer insights into material properties, design parameters, and device performance prediction or optimization. To find out how different factors affect device performance, parameter sensitivity analysis can be conducted. This involves altering the geometry of the device, the material properties, the operating environment, or the fabrication parameters, to pinpoint the main elements affecting performance. Additionally, simulations may reduce the necessity for iterative testing of the experiment, which can help with design optimization and cost. SCAPS enables detailed analysis of charge carrier dynamics by modeling the effects of varying doping concentrations on key parameters such as carrier mobility, recombination rates, and built-in electric field strength. Our simulations revealed that increasing the doping concentration enhanced carrier transport by improving the electric field, thereby facilitating charge separation and reducing recombination losses. However, excessive doping introduced mid-gap trap states, leading to higher Shockley–Read–Hall (SRH) recombination and a decline in open-circuit voltage (Voc). To ensure the broader applicability of our findings, we examine how the impact of doping concentration on recombination and carrier transport extended across various perovskite compositions and device architectures. Different perovskite formula-

tions, such as methylammonium lead iodide ($MAPbI_3$), formamidinium-based ($FAPbI_3$), and mixed halide compositions, exhibit distinct electronic properties, defect densities, and stability characteristics, which influence their response to variations in levels of doping. Using SCAPS-1D simulations, we assessed whether the observed trends held across these compositions by analyzing key performance metrics including open-circuit voltage (Voc), short-circuit current (Jsc), and fill factor (FF). Additionally, we explored how these effects may translate to different device architectures, such as planar and mesoporous structures, where charge transport mechanisms may differ. Our numerical and graphical analysis provides insights into the universality of our results, helping to guide doping strategies for optimizing diverse perovskite solar cell configurations in real-world applications.

5. Conclusions

Our findings demonstrate that the efficiency of perovskite-based solar cells can be further boosted through a bifacial structure. If copper oxide's effectiveness as an HTM is confirmed by experiments, it is possible that cells with a bifacial structure will perform even better. Furthermore, the device's longevity can be increased by shielding perovskite from moisture. Initial numerical analysis using SCAPS-1D suggested that the proposed structure could reach up to 31% power conversion efficiency. When illuminated from the p-side, efficiency increased by 22%, potentially achieving a total conversion efficiency of 33%. With material parameters taken from the pertinent literature, the computed BF for this structure was 71%. Consequently, the potential for developing functional n-i-p BPSCs is retained. However, it is worth noting that much of our research remains theoretical, and further experimental work is needed to validate the effectiveness of our proposed improvements. Nonetheless, our study provides valuable new insights for developing perovskite-based solar cells that are more robust and efficient, potentially resulting in significant advancements in the renewable energy sector.

Author Contributions: K.T.: writing—original draft, methodology, investigation, data curation, conceptualization; A.R.: writing—original draft, methodology, investigation, formal analysis, data curation; A.K.: investigation, formal analysis; P.C.: investigation, formal analysis; B.A.: investigation, formal analysis; M.I.H.: investigation, supervision, formal analysis. All authors have read and agreed to the published version of the manuscript.

Funding: This research was funded by High School Research Experience Project from Qatar Research, Development and Innovation, grant number HSREP05-0928-230013.

Data Availability Statement: The data that support the findings of this study are available from the corresponding author, M.I.H., upon reasonable request.

Acknowledgments: We would like to acknowledge the support from Hamad Bin Khalifa University.

Conflicts of Interest: The authors declare no conflicts of interest.

References

1. Grätzel, M. The light and shade of perovskite solar cells. *Nat. Mater.* **2014**, *13*, 838–842. [CrossRef] [PubMed]
2. Wei, Y.; Sun, X.; Meng, X.; Li, Z.; Zhang, L.; Zhou, K.; Ma, Z. Enhancing the properties of Cd-free MgZnS buffer for solar cells by co-sputtering ZnS and Mg targets. *Mater. Today Commun.* **2024**, *39*, 108766. [CrossRef]
3. Hossain, M.I.; Zakaria, Y.; Zikri, A.; Samara, A.; Aissa, B.; El-Mellouhi, F.; Hasan, N.S.; Belaidi, A.; Mahmood, A.; Mansour, S. E-beam evaporated hydrophobic metal oxide thin films as carrier transport materials for large scale perovskite solar cells. *Mater. Technol.* **2022**, *37*, 248–259. [CrossRef]
4. Hao, R.-M.; Zhu, L.; Shang, T.-F.; Xu, Z.-B.; Wu, Q.-P. Strong absorption of silica over full solar spectrum boosted by interfacial junctions and light–heat–storage of $Mg(OH)_2$–(CrO_x–SiO_2). *Chem. Eng. J.* **2024**, *497*, 154979. [CrossRef]

5. Noorasid, N.S.; Arith, F.; Mustafa, A.N.; Chelvanathan, P.; Hossain, M.I.; Azam, M.A.; Amin, N. Improved performance of lead-free perovskite solar cell incorporated with TiO_2 Electron Transport Layer and CuI Hole Transport Layer using SCAPs. *Appl. Phys.* **2023**, *129*, 132. [CrossRef]
6. Liang, M.; Ali, A.; Belaidi, A.; Hossain, M.I.; Ronan, O.; Downing, C.; Tabet, N.; Sanvito, S.; Ei-Mellouhi, F.; Nicolosi, V. Improving stability of organometallic-halide perovskite solar cells using exfoliation two-dimensional molybdenum chalcogenides. *npj 2D Mater. Appl.* **2020**, *4*, 40. [CrossRef]
7. Wang, E.; Chen, P.; Yin, X.; Gao, B.; Que, W. Boosting efficiency of planar heterojunction perovskite solar cells by a low temperature $TiCl_4$ treatment. *J. Adv. Dielectr.* **2018**, *8*, 1850009. [CrossRef]
8. Ghosh, P.; Sundaram, S.; Nixon, T.P.; Krishnamurthy, S. Influence of nanostructures in perovskite solar cells. In *Reference Module in Materials Science and Materials Engineering*; Elsevier: Amsterdam, The Netherlands, 2021.
9. Wang, D.-L.; Cui, H.-J.; Hou, G.-J.; Zhu, Z.-G.; Yan, Q.-B.; Su, G. Highly efficient light management for perovskite solar cells. *Sci. Rep.* **2016**, *6*, 18922. [CrossRef] [PubMed]
10. Yoo, G.Y. Broadband anti-reflective nanostructures by coating a low-index MgF_2 film onto a SiO_2 moth-eye nanopattern. *ACS Appl. Mater. Interfaces* **2020**, *12*. [CrossRef]
11. Zhao, P.; Yue, M.; Lei, C.; Lin, Z.; Su, J.; Chen, D.; Zhang, C.; Zhang, J.; Chang, J.; Hao, Y. Device Simulation of Organic–Inorganic Halide Perovskite/Crystalline Silicon Four-Terminal Tandem Solar Cell with Various Antireflection Materials. *IEEE J. Photovolt.* **2018**, *8*, 1685–1691. [CrossRef]
12. Arabatzis, I. Photocatalytic, self-cleaning, anti-reflective coating for photovoltaic panels: Characterization and moni-toring in real conditions. *Sol. Energy* **2018**, *159*, 251–259. [CrossRef]
13. Pan, Y.; Xin, C.; Wu, W.; Guan, M.; Wang, X. Microstructural and mechanical analyses of YBCO coated conductor tapes in high-irradiation environments. *Fusion Eng. Des.* **2025**, *211*, 114802. [CrossRef]
14. Elumalai, N.K.; Uddin, A. Hysteresis in organic-inorganic hybrid perovskite solar cells. *Sol. Energy Mater. Sol. Cells* **2016**, *157*, 476–509. [CrossRef]
15. Lin, L.; Jiang, L.; Li, P.; Fan, B.; Qiu, Y. A modeled perovskite solar cell structure with a Cu_2O hole-transporting layer enabling. *J. Phys. Chem. Solids* **2019**, *124*, 205–211. [CrossRef]
16. Middleton, W.M.; Van Valkenburg, M.E. Properties of Materials. In *Reference Data for Engineers*; Elsevier: Amsterdam, The Netherlands, 2002.
17. Song, Z.; Li, C.; Chen, L.; Yan, Y. Perovskite Solar Cells Go Bifacial—Mutual Benefits for Efficiency and Durability. *Adv. Mater.* **2022**, *34*, 2106805. [CrossRef] [PubMed]
18. Kumar, P.; Shankar, G.; Pradhan, B. Recent progress in bifacial perovskite solar cells. *Appl. Phys. A* **2023**, *129*, 63. [CrossRef]
19. Afzaal, M.; Karkain, S. Environmental Assessment of Perovskite Solar Cells. In *The Effects of Dust and Heat on Photovoltaic Modules: Impacts and Solutions*; Al-Ahmed, A., Inamuddin, Al-Sulaiman, F.A., Khan, F., Eds.; Springer: Berlin/Heidelberg, Germany, 2022; pp. 279–289.
20. Bal, S.S.; Basak, A.; Singh, U.P. Numerical modeling and performance analysis of Sb-based tandem solar cell structure using SCAPS—1D. *Opt. Mater.* **2022**, *127*, 112282. [CrossRef]
21. Baloch, A.A.B.; Hossain, M.I.; Tabet, N.; Alharbi, F.H. Practical Efficiency Limit of Methylammonium Lead Iodide Perovskite ($CH_3NH_3PbI_3$) Solar Cells. *J. Phys. Chem. Lett.* **2018**, *9*, 426–434. [CrossRef] [PubMed]
22. Belarbi, M.; Zeggai, O.; Louhibi-Fasla, S. Numerical study of Methylammonium Lead Iodide Perovskite solar cells using SCAPS-1D simulation program. *Mater. Today Proc.* **2022**, *51*, 2115–2119. [CrossRef]
23. Hossain, M.I.; Aissa, B.; Samara, A.; Mansour, S.A.; Broussillou, C.A.; Benito, V.B. Hydrophilic antireflection and antidust silica coatings. *ACS Omega* **2021**, *6*, 5276–5286. [CrossRef] [PubMed]
24. Salehi, H.; Eshaghi, A.; Rezazadeh, M.; Zabolian, H. Antireflective and anti-dust modified silica based thin film on solar cell cover glass. *J. Alloys Compd.* **2022**, *892*, 162228. [CrossRef]
25. Esfahani, M.B.; Eshaghi, A.; Bakhshi, S.R. Transparent hydrophobic, self-cleaning, anti-icing and anti-dust nano-structured silica based thin film on cover glass solar cell. *J. Non-Cryst. Solids* **2022**, *583*, 121479. [CrossRef]
26. Khattak, Y.H.; Vega, E.; Baig, F.; Soucase, B.M. Performance investigation of experimentally fabricated lead iodide perovskite solar cell via numerical analysis. *Mater. Res. Bull.* **2022**, *151*, 111802. [CrossRef]
27. Michaelson, H.B. The work function of the elements and its periodicity. *J. Appl. Phys.* **1977**, *48*, 4729–4733. [CrossRef]
28. Nath, B.; Ramamurthy, P.C.; Mahapatra, D.R.; Hegde, G. Electrode Transport Layer–Metal Electrode Interface Morphology Tailoring for Enhancing the Performance of Perovskite Solar Cells. *ACS Appl. Electron. Mater.* **2022**, *4*, 689–697. [CrossRef]
29. Nath, B.; Ramamurthy, P.C.; Hegde, G.; Mahapatra, D.R. Role of electrodes on perovskite solar cells performance: A review. *ISSS J. Micro Smart Syst.* **2022**, *11*, 61–79. [CrossRef]
30. Raza, E.; Ahmad, Z.; Asif, M.; Aziz, F.; Riaz, K.; Mehmood, M.Q.; Bhadra, J.; Al-Thani, N.J. Numerical Modeling and Performance Optimization of Carbon-Based Hole transport layer-Free Perov-skite Solar Cells. *Opt. Mater.* **2022**, *125*, 112075. [CrossRef]

31. Saha, P.; Halder, P.; Singh, S.; Bhattacharya, S. Optimization and Formulation of Different Hole-Transporting Ma-terials (HTMs) for the Performance of Eco-Friendly Cs_2TiBr_6-Based Perovskite Solar Cells. *Energy Technol.* **2024**, *12*, 2300991. [CrossRef]
32. Saha, P.; Singh, S.; Bhattacharya, S. Eco-Friendly Methyl-Ammonium Tin-Based Planar P–N Homojunction Perovskite Solar Cells: Design and Performance Estimation. *Int. J. Mod. Phys. B* **2023**, *37*, 22350169. [CrossRef]
33. Samantaray, M.R.; Rana, N.K.; Kumar, A.; Ghosh, D.S.; Chander, N. Stability study of large-area perovskite solar cells fabricated with copper as low-cost metal contact. *Int. J. Energy Res.* **2022**, *46*, 1250–1262. [CrossRef]
34. Shiraishi, M.; Ata, M. Work function of carbon nanotubes. *Carbon* **2001**, *39*, 1913–1917. [CrossRef]
35. Song, S.M.; Park, J.K.; Sul, O.J.; Cho, B.J. Determination of Work Function of Graphene under a Metal Electrode and Its Role in Contact Resistance. *Nano Lett.* **2012**, *12*, 3887–3892. [CrossRef] [PubMed]
36. Wang, M.; Liu, J.; Ma, C.; Wang, Y. Modular Perovskite Solar Cells with $Cs_{0.05}$ $(FA_{0.85}MA_{0.15})_{0.95}$ Pb $(I_{0.85}Br_{0.15})_3$ Light-Harvesting Layer and Graphene Electrode. *J. Electron. Mater.* **2022**, *51*, 2381–2389. [CrossRef]
37. Wu, Y.; Sun, X.; Dai, S.; Li, M.; Zheng, L.; Wen, Q.; Tang, B.; Yun, D.-Q.; Xiao, L. Broad-Band-Enhanced Plasmonic Perovskite Solar Cells with Irregular Silver Nanomaterials. *ACS Appl. Mater. Interfaces* **2022**, *14*, 16269–16278. [CrossRef]

Disclaimer/Publisher's Note: The statements, opinions and data contained in all publications are solely those of the individual author(s) and contributor(s) and not of MDPI and/or the editor(s). MDPI and/or the editor(s) disclaim responsibility for any injury to people or property resulting from any ideas, methods, instructions or products referred to in the content.